Mon. Not. R. Astron. Soc. **000**, 1–6 (2015) Printed 10 October 2015 (MN LATEX style file v2.2)

Red Supergiants as Cosmic Abundance Probes: NGC 2100

L. R. Patrick[1⋆], C. J. Evans[1,2], B. Davies[3], et al.
[1] *Institute for Astronomy, University of Edinburgh, Royal Observatory Edinburgh, Blackford Hill, Edinburgh EH9 3HJ, UK*
[2] *UK Astronomy Technology Centre, Royal Observatory Edinburgh, Blackford Hill, Edinburgh EH9 3HJ, UK*
[3] *Astrophysics Research Institute, Liverpool John Moores University, Liverpool Science Park ic2, 146 Brownlow Hill, Liverpool L3 5RF, UK*

Accepted Received 1; in original form

ABSTRACT
We have obtained KMOS spectroscopy for 17 red supergiant stars in the Large Magellanic Cloud (LMC) massive star cluster NGC 2100. Stellar parameters have been derived and are shown to ... compared to previous results.
Radial velocities are estimated for the targets ... .

Key words: Red Supegiants: stars.

1 INTRODUCTION

Something great about the LMC and how NGC 2100 fits into the mix. NGC 2100 is a young massive star cluster located on the near edge of the LMC, near the 30 Dor region. There have been many studies which have identified a large number of RSGs within the cluster. This is the first quantitative estimate of their metallicities.

Some NGC 2100 stats:
Age: 20 Myr (Niederhofer et al. 2015)
Mass: 4.36×10^4 (McLaughlin & van der Marel 2005)
R_{core} (pc): 3.03/0.99 (McLaughlin & van der Marel 2005)
Z: $log 0.007/Z_{\odot} = -0.34$ (Niederhofer et al. 2015)
V_{esc} (km s^{-1}): 7.9 (McLaughlin & van der Marel 2005)

Questions we would like to answer in this paper:
Are the known RSGs in this region genuine cluster members and if so what does their velocity dispersion look like?

How does the metallicity of these objects relate the to that in the nearby 30 Dor region and other RSGs within this galaxy?

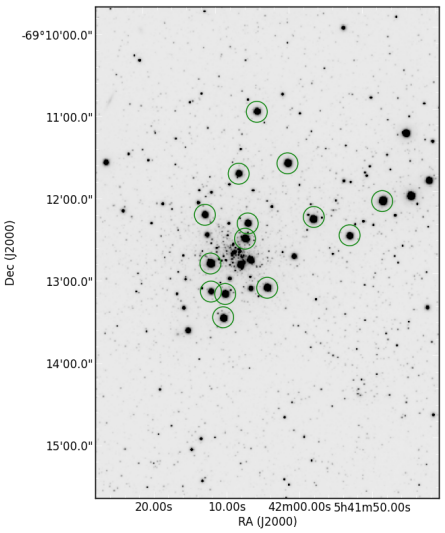

Figure 1. Positions of the NGC 2100 KMOS targets overlaid on a VISTA *J*-band image.

2 OBSERVATIONS AND DATA REDUCTION

2.1 Target Selection

- How were these targets selected?

2.2 KMOS Observations

These observations form part of the KMOS Gaurenteed Time Observing (PI: Evans) and were conducted in March 2015. The observations consist of 8×10 s exposures taken with the YJ grating with sky offset exposures (S) interleaved between the object (O) exposures in an O, S, O observing pattern. In addition, a standard set of KMOS calibration frames were also obtained as well as telluric standard frames using HIPXXX as the telluric standard star. Seeing conditions were stable at 1.0 arcseconds for the course of the observations.

The KMOS/esorex standard routines (Davies et al. 2013, SPARK;) were used to calibration and reconstruct the data cubes. Telluric correction was performed using the

⋆ E-mail: lrp@roe.ac.uk

24-arm telluric correction routine (described in detail in Patrick et al. (2015)). Briefly, corrections to the standard telluric recipe are put in place to correct for slight differences in wavelength calibration between the telluric and science spectra. This is implemented using an itertive cross-correlation approach. Additionally, differences in the strength of the telluric features are corrected by apply a simple scaling. Once these corrections are in place, the scicence spectra are divided by the appropriate telluric spectrum for that particular IFU.

2.3 Data Reduction

3 RADIAL VELOCITIES

Radial velocities are estimated using an iterative cross-correlation method. To ensure the KMOS spectra are at rest wavelength, the observed spectra are first cross-correlated against a model telluric spectrum, taken from the ISSAC web-pages, which is known to be at a much higher resolution than that of the observations. This cross-correlation is performed in the $1.15 - 1.17\,\mu$m region as this is where the telluric features dominate.

Once the observed spectra are at rest wavelength, an initial guess of the radial velocity is estimated by cross-correlating the science spectra with an appropriate synthetic RSG spectrum in the $1.17-1.21\,\mu$m region. This wavelength regime is selected based on the dominance of atomic features in the RSG spectrum at these wavelengths. To increase reliability, this initial guess is improved upon by using five carefully selected groups of stellar absorption lines centred on some of the strongest atomic features in this region. These lines and regions are selected based on their reliability and are known to be not affected by telluric absorption. Figure 2 illustrates which features have been used for the analysis.

Radial velocities are independently calculatedfor each of region by means of iterative cross-correlation. This results in five estimates of the radial velocity for each star which are then compared and any region which produces a radial velocity which is an obvious outlier to the distribution is rejected. The final radial velocity for each star is the mean of the distribution resulting from the (non-rejected) regions. The error on this mean is calculated by taking the standard deviation of the data, normalised by the number of regions used ($err = \sigma/N_{regions}$). This method is shown to work well for KMOS spectra (Lapenna et al. 2015; Patrick et al. 2015).

Figure 3 shows the radial velocities for all targets as a function of distance from the centre of the cluster, shown alongside the systemic radial velocity of the LMC (green dashed line; see section 5 for a discussion on this).

An upper limit to the line-of-sight velocity dispersion can calculated using the equations,

$$\mu = \frac{1}{\sum_i 1/\sigma_i^2} \sum_i \frac{RV_i}{\sigma_i}, \tag{1}$$

$$Var = \frac{1}{\sum_i 1/\sigma_i^2} \sum_i \frac{(RV_i - \mu)^2}{\sigma_i^2}, \tag{2}$$

$$\sigma_{1D} = \sqrt{Var \frac{N}{N-1}} \tag{3}$$

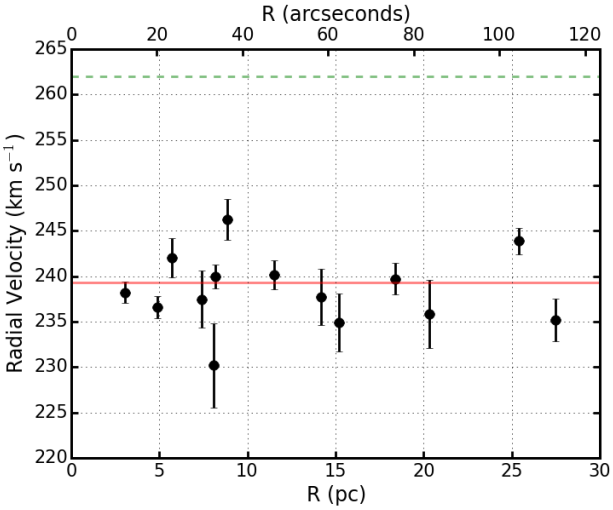

Figure 3. Radial velocities of KMOS targets shown as a function of distance from the cluster centre. Green dashed line shows the LMC systemtic veloctiy ($262.2 \pm 3.4\,$km s^{-1}; McConnachie 2012) and the solid red line shows the mean of the sample ($248 \pm 17\,$km s^{-1}).

where σ_i is the uncertainty on the radial velocity measurement RV_i and N is the number of stars in the sample (Hénault-Brunet et al. 2012, and references therin).

Using σ_{1D} as an upper limit on the velocity distribution, one can calculate the dynamical/virial mass of the cluster using the equation,

$$M_{vir} = \frac{\eta \sigma_{1D}^2 r_{eff}}{G} \tag{4}$$

where M_{vir} is the virial mass, $\eta = 6r_{vir}/r_{eff} = 9.75$ providing the density profile of the cluster is sufficently steep (Portegies Zwart et al. 2010). However, NGC 2100 has a relatively shallow density profile ($\gamma = 2.3$) which means $\eta > 9.75$ therefore the estimate of M_{vir} is knowingly an overestimate. Using this wq

4 STELLAR PARAMETERS

Stellar paramaeters are estimated using the J-band analysis technique descibred initially in Davies et al. (2010) and tested rigorously in Gazak et al. (2014) and Davies et al. (2015). These studies show that using a narrow spectral window within the J-band one can accurately derive global metallicitiy ([Z]) to within $\pm 0.2\,dex$ at the resolution of KMOS observations with S/N $\geqslant$ 100. The ranges of each parameter for the grid of model spectra are listed in table 2.

- Stellar parameters for all targets are listed in table 3.
- How do we know these parameters are ligit?
- Compare to Ben's implemenation
- find some previous studies of young stars in this cluster

Stellar parameters have been derived using the J-band analysis technique described in Davies et al. (2010). This however, includes the affects of magnesium in the analysis by using two strong magnesium absorption lines which are

Table 1. Summary of VLT-KMOS targets in NGC 6822.

ID	S/N	α (J2000)	δ (J2000)	B	V	I	J	H	K_s	RV (km s^{-1})	Notes
0207-0134568	318	05:41:47.873	-69:12:05.959	16.488	13.749	9.769	9.525	8.603	8.200	233.989	
0207-0134683	198	05:41:52.430	-69:12:30.410	16.430	14.267	11.970	10.413	9.526	9.155	213.781	
0207-0134811	202	05:41:57.286	-69:12:16.480	14.074	13.019	11.170	9.811	9.036	8.738	253.005	
0207-0134979	252	05:42:03.877	-69:13:07.410	15.624	13.579	11.410	9.839	8.996	8.740	246.637	
0207-0135059	196	05:42:06.348	-69:12:20.150	00.000	00.000	11.810	10.371	9.480	9.159	248.928	
0207-0135069	256	05:42:06.764	-69:12:31.245	15.643	13.675	11.390	9.977	9.150	8.807	245.703	
0207-0135150	240	05:42:09.647	-69:13:11.263	15.367	13.383	11.370	9.976	9.136	8.841	247.856	
0207-0135162	250	05:42:10.001	-69:13:28.210	16.060	13.827	11.580	10.021	9.150	8.823	246.984	
0207-0135205	304	05:42:11.574	-69:12:48.770	16.327	14.033	11.450	9.557	8.617	8.264	245.22	
0207-0135206	151	05:42:11.592	-69:13:09.257	16.165	14.272	12.340	10.943	10.090	9.788	232.663	
0207-0135220	195	05:42:12.182	-69:12:13.144	15.483	13.606	11.750	10.440	9.622	9.335	290.345	
0208-0135292	262	05:42:00.722	-69:11:36.925	15.579	13.674	9.421	9.900	9.017	8.683	246.551	
0208-0135383	211	05:42:04.762	-69:10:58.816	15.550	13.800	12.770	10.319	9.427	9.159	252.045	
0208-0135446	201	05:42:07.435	-69:11:43.692	15.531	13.661	11.780	10.482	9.610	9.351	271.205	

Photometric data taken from the SIMBAD database. Typical errors on photometric data: 0.026, 0.014, 0.04, 0.024, 0.026, 0.022 respectively. Near-IR data taken from 2MASS.

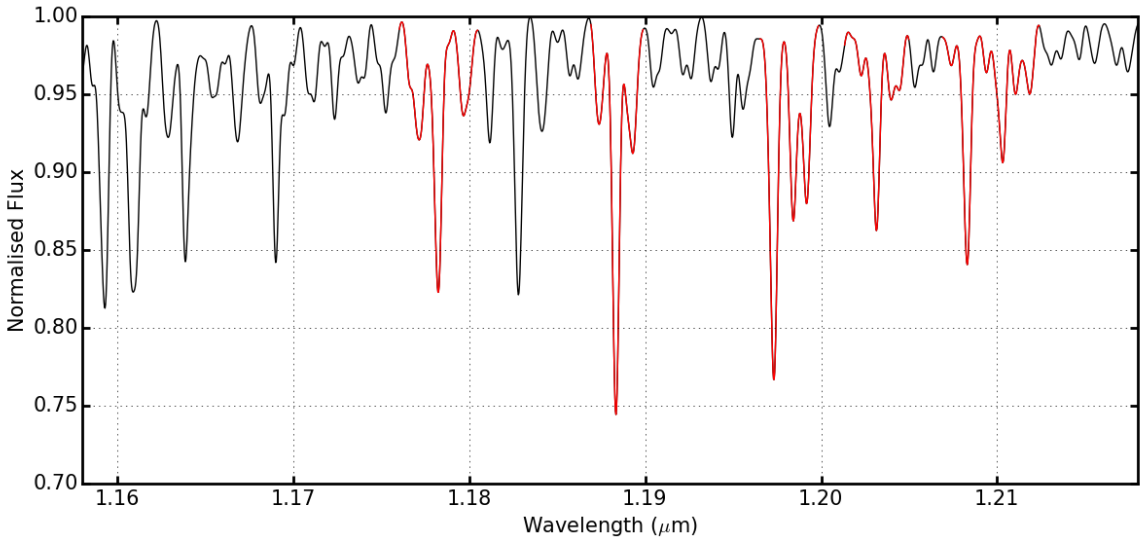

Figure 2. Sythetic RSG spectrum used calcualte the radial velocities for programme stars. Red regions illustrate regions where a cross-correlation is performed between the observed spectra and this synthetic spectrum. These regions provide consistent results with an average dispersion between the five regions of of 2.3 km s^{-1}.

known to be affected strongly by non-LTE effects (Bergemann et al. 2015). In order to use these lines Bergemann et al. (2015) calcualte non-LTE corrections for these magnesium lines. This also allows one to derive a metallicitiy based solely on the α elements allowing one to derive the [α/Fe] ratio. This is the first time which this technique has been used to estimate this parameter. The parameters fitted are defined in table

- Comparisons to previous studies of young stars in this region
- Compare to LMC-wdie studies of young stars
- How does it compare to Davies et al. 2015? Do I also see this slightly high Z?
- Is this cluster special?
- We know it is young and massive in one of the most vigously star forming regions in the local universe

Table 2. Model grid used for analysis. **This needs to be updated for new grids!**

Model Parameter	Min.	Max.	Step size
T$_{eff}$ (K)	3400	4000	100
	4000	4400	200
[Z] (dex)	-1.50	1.00	0.25
log g (cgs)	-1.0	1.0	0.5
ξ (km s^{-1})	1.0	6.0	1.0

5 DISCUSSION

- What does this mean for stellar evolution models?
- Can we say anything interesting about what α should be?
- Will we have α at all?
- Do these Teff's fit into the picture?
- Can we believe the Z's?

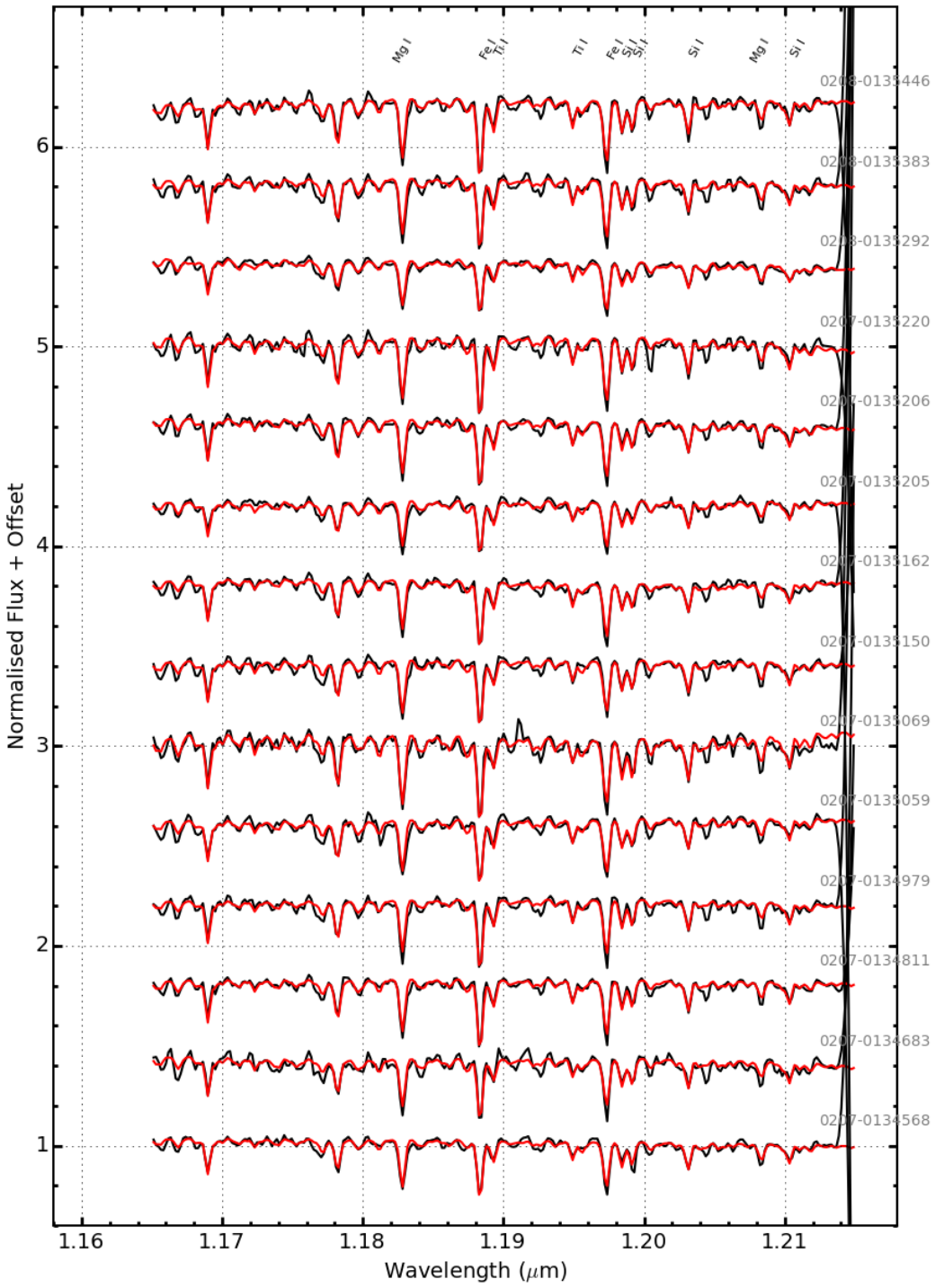

Figure 4. KMOS spectra of the NGC 6822 RSGs and their associated best-fit model spectra (black and red lines, respectively). The lines used for the analysis from left-to-right by species are: Fe I$\lambda\lambda$1.188285, 1.197305, Si I$\lambda\lambda$1.198419, 1.199157, 1.203151, 1.210353, Ti I$\lambda\lambda$1.189289, 1.194954. The two strong Mg I lines are also labelled, but are not used in the fits (see Section **??**).

Table 3. Fit parameters for NGC 2100 KMOS targets

Target	IFU	ξ (km s^{-1})	[Z]	log g	T$_{eff}$ (K)
0207-0134568	#	4.0 ± 0.3	-0.40 ± 0.15	0.4 ± 0.3	3890 ± 70
0207-0134683	#	3.5 ± 0.2	-0.79 ± 0.09	-0.5 ± 0.11	3800 ± 40
0207-0134811	#	5.0 ± 0.2	-0.30 ± 0.14	-0.10 ± 0.4	3980 ± 60
0207-0134979	#	4.3 ± 0.3	-0.48 ± 0.15	-0.10 ± 0.4	3840 ± 70
0207-0135059	#	3.0 ± 0.6	-0.68 ± 0.35	-0.13 ± 0.4	3720 ± 80
0207-0135069	#	4.7 ± 0.2	-0.63 ± 0.13	-0.7 ± 0.28	3700 ± 40
0207-0135150	#	4.0 ± 0.2	-0.52 ± 0.14	-0.10 ± 0.4	3720 ± 70
0207-0135162	#	5.0 ± 0.0	-0.96 ± 0.0	-0.5 ± 0.0	3520 ± 00
0207-0135205	#	3.8 ± 0.3	-0.61 ± 0.19	-0.5 ± 0.5	3600 ± 70
0207-0135206	#	3.13± 0.4	-0.57 ± 0.31	0.13 ± 0.4	3630 ± 70
0207-0135220	#	3.3 ± 0.3	-0.54 ± 0.17	0.3 ± 0.5	3940 ± 80
0208-0135292	#	4.0 ± 0.2	-0.74 ± 0.16	-0.6 ± 0.4	3710 ± 70
0208-0135383	#	4.18± 0.3	-0.62 ± 0.17	-0.10 ± 0.4	3690 ± 60
0208-0135446	#	4.05± 0.3	-0.49 ± 0.18	-0.05 ± 0.5	3730 ± 70

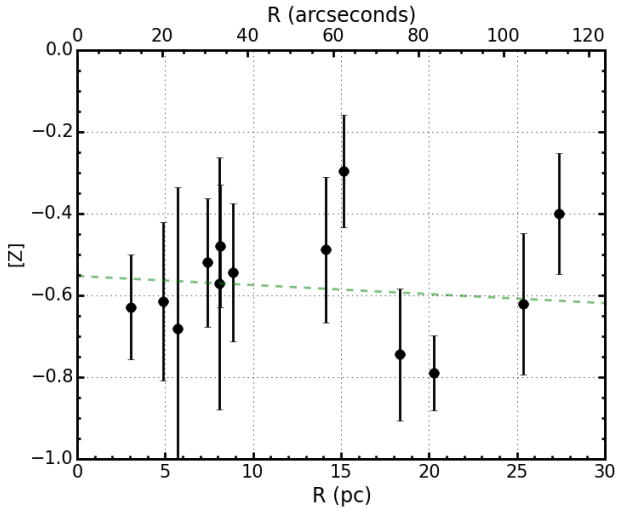

Figure 5. Estimated metallicities shown against distance from the centre of the cluster.

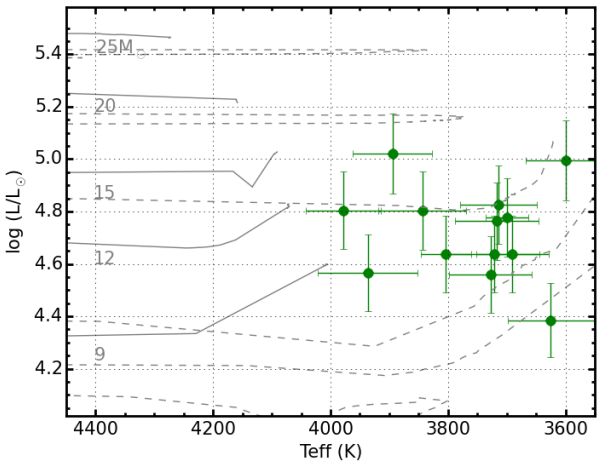

Figure 6. Estimated metallicities shown against distance from the centre of the cluster.

- Can we say anything about an age spread? (Niederhofer et al. 2015)
- e.g. is the distribution of masses what we would expect from a single stellar population?
-

6 CONCLUSIONS

ACKNOWLEDGMENTS

...

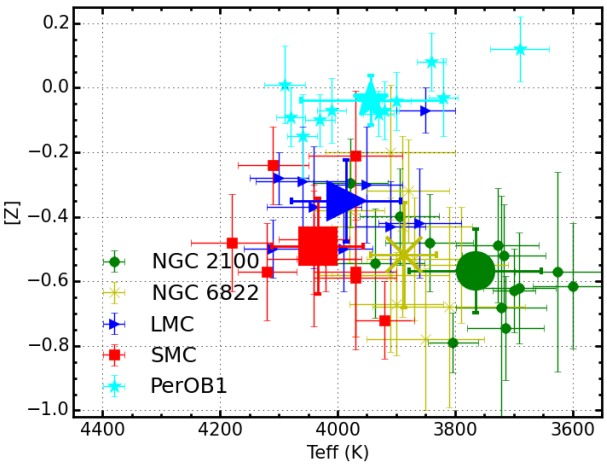

Figure 7. Estimated metallicities shown against estimated effective temperature.

REFERENCES

Bergemann, M., Kudritzki, R.-P., Plez, B., et al. 2012, ApJ, 751, 156
Bergemann, M., Kudritzki, R.-P., Würl, M., et al. 2013, ApJ, 764, 115
Bergemann, M., Kudritzki, R.-P., Gazak, Z., Davies, B., & Plez, B. 2015, ApJ, 804, 113
Davies, B., Kudritzki, R.-P., & Figer, D. F. 2010, MNRAS, 407, 1203

Davies, B., Kudritzki, R.-P., Gazak, Z., et al. 2015, ApJ, 806, 21
Davies, R. I., Agudo Berbel, A., Wiezorrek, E., et al. 2013, A&A, 558, A56
Gazak, J. Z., Davies, B., Kudritzki, R., Bergemann, M., & Plez, B. 2014, ApJ, 788, 58
Gazak, J. Z., Davies, B., Bastian, N., et al. 2014, ApJ, 787, 142
Hénault-Brunet, V., Evans, C. J., Sana, H., et al. 2012, A&A, 546, A73
Lapenna, E., Origlia, L., Mucciarelli, A., et al. 2015, ApJ, 798, 23
McConnachie, A. W. 2012, AJ, 144, 4
McLaughlin, D. E., & van der Marel, R. P. 2005, ApJS, 161, 304
Niederhofer, F., Hilker, M., Bastian, N., & Silva-Villa, E. 2015, A&A, 575, A62
Patrick, L. R., Evans, C. J., Davies, B., et al. 2015, ApJ, 803, 14
Portegies Zwart, S. F., McMillan, S. L. W., & Gieles, M. 2010, ARA&A, 48, 431